Pierre Auger Project Note: GAP-97-071

Study of Auger Ground Array Performance using Parametric Showers

Michael S. Gold, Jason Jordan and John A.J. Matthews
New Mexico Center for Particle Physics
University of New Mexico
Albuquerque, NM 87131

November 1, 1997

Abstract

Hillas observed that the particle density, ρ, several hundred meters from the core of an extensive air shower provides a measure of the shower energy that is relatively insensitive to the depth of initial interaction and to initial composition. This note uses the Haverah Park parameterization for extensive air showers detected in 1.2m deep water Cherenkov tanks and a model of the Auger ground array to study the measurement precision of $\rho(r)$. Parameters that are varied include:

- ground array geometry,
- tank spacing,
- tank signal threshold and overflow values,
- magnitude of tank to tank gain variations,
- vertical equivalent muon (VEM) statistical significance factor,
- shower zenith angle, and
- shower energy.

1. Introduction

Michael Hillas [1] observed that the particle density, ρ, several hundred meters from the core of an extensive air shower provides a measure of the shower energy that is relatively insensitive to the depth of the initial cosmic ray interaction in the atmosphere and to the initial composition of the cosmic rays. As proposed [2], the Auger ground array will follow the Haverah Park experiment and measure the particle density in Vertical Equivalent Muons (VEM) using the signal from 1.2m deep water Cherenkov tanks.

The energy uncertainty from the Auger ground array can then be divided into three separate factors:

- variations in ρ from variations in the depth of the initial interaction and from shower to shower variations in the particle nature of the cosmic ray (*i.e.* composition effects),
- errors in the measurement of ρ as reconstructed from the sparse ground array data, and
- errors in the conversion factor between ρ and the initial cosmic ray energy.

The variation in ρ from variations in the depth of the initial interaction and from compositional variations in the cosmic rays are minimized when the atmospheric depth of the average shower in the the ground array occurs near the *maximum* of the curve of ρ *versus* shower depth [3]. This is set by the atmospheric depth of the site and by the range of cosmic ray energies to be studied. We denote these uncertainties as *shower depth* uncertainties.

In addition to the shower depth uncertainties in ρ, a sparse ground array reconstructs the lateral distribution function (ldf) of the shower only to some level of precision. We denote the uncertainties from the reconstruction as *measurement* uncertainties. At a minimum the measurement uncertainties are set by the optimization and performance capabilities of the ground array. This is the focus of the present note. The minimum measurement uncertainties may be increased by fluctuations in the shower ldf, *e.g.* from lack of azimuthal symmetry in showers or from unusual showers with a ldf very different from the average shower (with the same energy and zenith angle). Although there is no evidence for this in extreme high energy data [4,8], maybe a study needs to be done.

Finally there are uncertainties in the conversion factor between ρ and the initial cosmic ray energy. We denote this uncertainty as the *conversion factor* uncertainty. The conversion factor uncertainty is mainly an overall systematic error between experiments. However changes in the cosmic ray composition over the energy range of a given experiment will add to the uncertainties between different energy points in the data of a given experiment. The conversion factor is obtained from full shower plus detector simulations using detailed Monte Carlo programs [5] or from cross calibration of the ground array using air Cherenkov [6] or

fluorescence signals from a pool of common events as proposed for the Pierre Auger experiment. For extreme high energy cosmic rays the level of disagreement between experiments indicates that the conversion factor uncertainty is typically $\leq 20\%$ [7].

In this study we vary parameters of the Auger ground array to study the relationship between the parameters of the ground array and the *measurement* uncertainties from the ground array. The quantities studied include: shower energy resolution, offsets in the reconstructed shower energy, resolution in the location of the shower core and resolution in the exponent of the ldf. Ground array parameters that are varied include:

- ground array geometry,
- tank spacing,
- tank signal threshold and overflow values,
- magnitude of tank to tank gain variations,
- vertical equivalent muon (VEM) statistical significance factor,
- shower zenith angle, and
- shower energy.

2. Auger Ground Array Simulation Model

To parameterize the ldf of showers in the Auger ground array we assume the Haverah Park lateral distribution function [8,9]. This is shown in Fig. 1 for showers in the energy range of this study and at the showers' average zenith angle of $\sim 30°$. Detailed shower Monte Carlo simulations [2] indicate that this assumption may underestimate the signal by a factor of ~ 2. Thus our performance estimates are conservative as our energy scale may then be high by a similar factor.

The simulation and analysis of extensive air showers in the Auger ground array is done as follows:

a) *Simulation of Cherenkov Tank Signals*: Events of a given energy and angle are generated with core locations distributed uniformly over the Auger array (but away from the array boundaries). The magnitude of the tank signals are then used to reconstruct the impact point, *i.e.* shower core location, the shower energy and the exponent of the lateral distribution function. This is the focus of the present study. The tank timing information is used to determine the shower direction to $< 2°$ [2]. For modest

zenith angles, $\theta \leq 45°$, the uncertainty in the shower energy from the uncertainty in the shower direction is small [10] and we ignore it in this study.

The tanks are placed on a uniform grid, either hexagonal or square. For the square grid the tank separation is scaled to the hexagonal separation with the same effective area per tank:

$$d^2_{square} \quad = \quad \frac{\sqrt{3}}{2} \cdot d^2_{hexagon}$$

In this note all distances are quoted in *hexagonal* grid units. Thus the design report tank separation of 1500m (hexagonal geometry) corresponds to an equivalent separation of 1396m for a square geometry.

The average tank signal is taken as the tank area (10m^2) times the ldf (VEM/m^2) at the location of the tank center; see Fig. 1. Thus no zenith angle correction is made to the tank signals. Actual tank signals are obtained from the average signals following Poisson statistics. Because the water Cherenkov tanks measure both the local electromagnetic energy and a weighted signal from the through-going muons, the statistical significance of a measurement is greater than $\sqrt{\overline{N}}$ where $\overline{N}$ is the average signal in VEMs [8]. Following Ref. 8 we include a statistical significance factor, f_s, where the statistical uncertainty in $\overline{N}$ is then:

$$\delta\overline{N} \quad = \quad \sqrt{f_s \cdot \overline{N}}$$

In the Haverah Park experiment $f_s = 0.4$. This factor is included in the Poisson statistics by taking the Poisson average signal as $\overline{N}/f_s$ and then scaling the Poisson distributed output by f_s to obtain the tank signal, N. In addition the tank signals are smeared assuming tank to tank response nonuniformities, $\delta N/N \quad = \quad \sigma_g$. In the Haverah Park experiment $\sigma_g = 0.05$ [8]. Finally the uncertainty in a tank signal, needed for the χ^2 fit, is taken as:

$$\delta N \quad = \quad \sqrt{(f_s^2 \cdot (\frac{\overline{N}}{f_s} + 1)) \quad + \quad (\sigma_g \cdot N)^2}$$

where the "+1" is an empirical correction between Poisson statistics and Gaussian errors for $\overline{N}/f_s \sim 1$.

b) *χ^2 Fit to Shower Lateral Distribution Function*: Showers with ≥ 4 tanks with signals $N_{min} \leq N \leq N_{max}$ are fitted [11] to the Haverah Park ldf with four free parameters: the location of the shower core, $(x, y)_{core}$, the normalization, k, and the radial exponent, η, where:

$$\rho(r) \quad = \quad k \cdot r^{-(\eta + \frac{r}{4000m})} \qquad\qquad (r < 800m)$$

and

$$\rho(r) \quad = \quad k \cdot r^{-(\eta + \frac{r}{4000m})} \cdot (\frac{r}{800m})^{1.03} \qquad\qquad (r \geq 800m)$$

For tank signals where $\overline{N} < N_{min}$, the $N \geq N_{min}$ requirement can result in systematic shifts in the fitted value for η (*i.e.* systematically favoring values of η less than the true or input value). Thus fits were also done including tanks that failed the $N \geq N_{min}$ selection but where the tank distance from the shower core was less than the maximum distance to a tank that passed the $N \geq N_{min}$ selection.

c) *Errors Determined by the Simulation*: Typically 1000 events are simulated for a given *point* in parameter/variable space. The parameter space includes both quantities describing the shower, *e.g.* shower energy and angle, as well as quantities that describe the Auger ground array, *e.g.* tank separation, tank geometry, shower thresholds, value for the VEM statistical significance factor and tank to tank gain variations [12]. To *control* the large number of variables, we define a set of *default* parameters. Studies are then done varying one of the parameters at a time. The list of default parameters as well as the range for each parameter is given in Table 1. Of the default parameters a tank to tank gain uncertainty of 5% [12] and a variable f_s factor would probably be more realistic. For large tank signals these two changes partially compensate one another. The maximum tank signal, $N_{max} = 2000$ VEMs, was set by the requirement that not more than one tank exceed N_{max} at the largest shower energy, 2×10^{20} eV. The minimum tank signal, N_{min}, was set to ~ 1 VEM corresponding to one (actual) muon/tank at large distances from the show core.

One final selection also needs to be applied, at least for some of the possible Auger ground arrays. This selection is to exclude showers that will not reconstruct well to a four parameter ldf fit. The problem showers are those with cores close to a tank. The problem is not (only) that the nearest tank is saturated, but that for such showers the distances to the non-saturated tanks fall into clusters with tanks in a given cluster having very similar distances to the shower core. The distance to the 1^{st} cluster is approximately the tank separation. In the hexagonal array the distance to the 2^{nd} cluster is $\sqrt{3}$ times the tank distance; in the square array the distance to the 2^{nd} cluster is is $\sqrt{2}$ times the tank distance, and so on. In a sparse array the distance to the 2^{nd} cluster of tanks can be sufficiently great that few or no tanks in the 2^{nd} cluster pass the minimum threshold selection. In this case the tank data constrains the magnitude of the ldf at $r \approx$ tank separation but the data provides little information on the radial derivative of the ldf. Thus η is essentially defined by the tank uncertainties. This problem is simply solved by excluding showers with cores within some distance of a tank. Empirically, the removal of $\sim 10\%$ of the events results in a significant reduction of the measurement errors. Thus for this study we do two analyses: one for all showers, and one for events with reconstructed core locations $\geq d_{cut}$ from any tank; see Table 1 for d_{cut} values.

The distribution of the $input - fit$ quantity, *e.g.* $x_{core}^{input} - x_{core}^{fit}$, is then used to evaluate the ground array measurement RMS errors and the systematic OFFSETs in the given quantity. This approach is used to determine the ground array measurement error of the shower core location and for the ground array measurement error of the radial exponent of the ldf, η.

To determine the RMS errors and systematic OFFSETs for the shower energy, we assume that $\rho(r)$ is linearly related to the shower energy. Then $\delta E/E = \delta\rho(r)/\rho(r)$ where $\delta\rho(r)/\rho(r)$ is given by $(\rho(r)^{input} - \rho(r)^{fit})/\rho(r)^{input}$. In this study the functional form for the ldf used in the fit is the same as the input form. In practice Auger hybrid events will be used to determine experimentally the ldf at Auger energies and for the Auger water Cherenkov detectors. Nevertheless, when we assume perfect knowledge of the ldf the resulting errors are a lower bound on the actual experimental errors.

3. Simulation Results

As noted above, simulations were done over the range of parameters summarized in Table 1. Modest variations in several of the parameters did not result in significant changes in the reconstruction of the showers. These parameters included shower zenith angle, N_{max}, N_{min}, and σ_g. In general excluding showers that reconstructed within a distance, d_{cut}, of a tank significantly reduced the reconstruction uncertainties for the hexagonal geometry ground array. Thus for the hexagonal geometry a somewhat arbitrary choice was made to exclude $\sim 10\%$ of the showers, corresponding to $d_{cut} = 250$m for a tank separation of 1500m, even though a larger exclusion region would have reduced the uncertainties further. Finally the VEM statistical significance factor, f_s, was set to the Haverah Park value of 0.4 [8] and was taken to be independent of distance from the shower core. As noted above our somewhat aggressive (*i.e.* low) value for σ_g partially compensated for the fact that f_s was unlikely to be constant and was probably significantly less than the Haverah Park value close to the shower core where the signals were largest. As a cross check simulations were done with a variable f_s, see Table 1, and simultaneously $\sigma_g = 5\%$, and were consistent with the results quoted below.

The major results of the simulation study are as follows:

a) *Average number of good tanks versus shower energy*: The average number of tanks with a signal, N, between $N_{max} \geq N \geq N_{min}$ are shown as a function of shower energy in Fig. 2a. The average signal, N, was $10\times$ the particle density shown in Fig. 1. As noted above, for tank signals near threshold the $N \geq N_{min}$ requirement can result in systematic shifts in the fitted value for η (*i.e.* systematically favoring values of η less than the true or input value). Thus fits were also done including tanks that failed the $N \geq N_{min}$ selection but where the tank distance from the shower core was less than the maximum distance to a tank that passed the $N \geq N_{min}$ selection. The average number of tanks in this case is shown in Fig. 2b. The results for both square and hexagonal geometries are essentially identical. In addition the results in Fig. 2b are in good agreement with simulations reported in the Pierre Auger design report [2].

b) *Uncertainty in reconstructed core location*: As noted above the simulated tank signals are fit to the input Haverah Park ldf. Four parameters are determined: x_{core}, y_{core},

k, and η. The uncertainties in x_{core} as a function of the shower energy are shown in Fig. 3a and b. The results for y_{core} are essentially the same. The x_{core} resolution is seen to be rather similar for hexagonal and square arrays. The main difference is that all events are included for the square array whereas only $\sim 90\%$ of the events are included for the hexagonal array. We note that the resolution in x_{core} does degrade below $\sim 5 \times 10^{19}$eV.

The uncertainties in x_{core} as a function of the tank separation distance are shown in Fig. 4a and b for 5×10^{19}eV showers. The trend is for the x_{core} uncertainty to increase as the tank separation increases. There is nothing unusual about the 1500m separation in the design report. The hexagonal geometry simulation shows some improvement in resolution for fits where tanks below threshold (see above and figure caption) are included in the fit.

c) *Uncertainty in reconstructed radial exponent, η*: The uncertainties in the radial exponent, η, as a function of the shower energy are shown in Fig. 5a and b. The results are similar to the results for the x_{core} reconstruction with the square array providing equal or better performance with respect to the hexagon array. As with the x_{core} study, the resolution in η is observed to degrade below $\sim 5 \times 10^{19}$eV.

The uncertainties in η as a function of the tank separation distance are shown in Fig. 6a and b for 5×10^{19}eV showers. As with the x_{core} study, the uncertainty in η increases as the tank separation increases. There is nothing unusual about the 1500m separation in the design report for the square geometry. The hexagonal geometry simulation shows significant improvement in resolution for fits where tanks below threshold (see above and figure caption) are included in the fit and when showers with reconstructed core distances less than d_{cut} from a tank are excluded.

d) *Shower energy resolution*: As noted above the shower energy is based on comparing the reconstructed particle density, $\rho(r)^{fit}$, with the input distribution, $\rho(r)^{input}$, at various distances, r, from the reconstructed shower core. Results are shown as a function of energy in Fig. 7a and b for the hexagonal geometry and in Fig. 7c and d for the square geometry. Each figure reports results at three distances: $r = 1000$m, $r = 1200$m and $r = 1400$m. The best resolution is obtained at a distance of $1200 \sim 1400$m. The square geometry prefers a somewhat smaller radius and the hexagonal geometry a somewhat larger radius. The energy resolution is observed to degrade below $\sim 5 \times 10^{19}$eV.

The shower energy resolutions as a function of the tank separation distance are shown in Fig. 8a and b for 5×10^{19}eV showers. Unlike the results in Fig. 7 which are determined at fixed distances from the shower core, the energy resolution results in Fig. 8 allow for the energy to be determined at increasing distances from the shower core as the tank separation increases. In all cases the best resolution is reported. Results based on evaluating the energy at a fixed radial distance from the shower core would show a more rapid degradation of the resolution with increasing tank separation than in this figure. In general the square geometry resulted in a somewhat better energy resolution, and performed better when this study was done using a fixed distance, $r = 1200m$,

from the shower core (not shown) than the hexagonal geometry. As with the x_{core} and η studies, the energy resolution degrades as the tank separation increases. There is nothing unusual about the 1500m separation in the design report.

e) $\underline{E^{fit}_{shower}/E^{input}_{shower}}$: In addition to the rms scatter in the reconstructed shower energy, part d) above, it is important to know if there are systematic offsets in the reconstructed shower energy. The results for $E^{fit}_{shower}/E^{input}_{shower}$ are shown in Fig. 9a and b for the hexagonal geometry and in Fig. 9c and d for the square geometry. The addition of tanks that failed the $N \geq N_{min}$ selection, but where the tank distance from the shower core was less than the maximum distance to a tank that passed the $N \geq N_{min}$ selection, resulted in $E^{fit}_{shower}/E^{input}_{shower}$ values significantly closer to 1.0 for both hexagonal and square geometries. Systematic offsets were small except at the lowest energies $1 \sim 2 \times 10^{19}$eV.

4. Summary

This simulation study shows that the Pierre Auger ground array with a tank spacing of 1500m, based on hexagonal geometry, will provide uniform response for showers $\geq 5{\times}10^{19}$eV. The precise value of this energy depends on more sophisticated simulations.

Detailed comparisons of hexagonal versus square geometry for the Auger ground array find in all cases better performance with the square array. Thus based on this study we recommend changing the Auger baseline design from a hexagonal to a square geometry for the ground array.

In addition to the shower depth uncertainties in ρ, a sparse ground array reconstructs the lateral distribution function (ldf) of the shower only to some level of precision. The design and performance of the ground array will naturally result in an optimal distance, r_{opt}, from the shower core where the experimentally determined value for $\rho(r)$ is closest to the actual particle density. The present study finds that r_{opt} is $\sim$ 1200m for the design tank spacing of 1500m.

Studies of the array performance as a function of the tank spacing find a monotonic degradation of performance with increasing tank separation. The 1500m tank separation in the design report is not near any *cliff*. Thus can the separation be increased significantly? While this is a topic for a separate study, we can make some observations from the present study:

- For tank spacings of 1500m, based on hexagonal geometry, all resolutions were observed to degrade significantly below shower energies of $\sim 5 \times 10^{19}$eV [1].
- Thus above this energy the ground array resolutions are approximately constant.
- This energy will increase for tank spacings > 1500m.
- The calibration of the ground array using hybrid events will be most reliable in the energy region where the ground array performance is approximately constant; in this study this is an energy of $\geq 5 \times 10^{19}$eV.
- Ideally the ground array calibration should not be limited by hybrid statistics. As the minimum energy of *good* calibration events increases the integral number of events varies approximately as $E^{-2}_{minimum}$. This sets the maximum energy for the start of the "approximately constant" performance domain of the ground array and thus also the maximum tank separation for the ground array.
- Given the modest hybrid data samples expected in Auger at energies $> 2 \sim 5 \times 10^{19}$eV only modest or perhaps no increases in the ground array tank separation may be possible.

[1] As noted previously, the energy scale in this simulation may be as much as a factor of 2 high. The point is that there is an energy, probably between $2 \sim 5 \times 10^{19}$eV, where the ground array resolutions degrade significantly.

References

[1] A. M. Hillas, et al, 12th I.C.R.C., **3**, 1001 (1971)

[2] Pierre Auger Collaboration, *The Pierre Auger Observatory Design Report*, March 14, 1997

[3] J. A. J. Matthews, *Back of the Envelope Insights into Shower Energy Measurements by Sparse Ground Arrays*, GAP Note GAP-97-018 (1997)

[4] S. Yoshida et al, J. Phys. **G20**, 651 (1994);
M. Nagano, private communication

[5] R.S. Fletcher et al, Phys. Rev. **D50**, 5710 (1994);
A.M. Hillas, 24th I.C.R.C., **1**, 270 (1995)

[6] M.N. Dyakonov et al, 22th I.C.R.C., **2**, 93 (1991);
A.J. Bower et al, J. Phys. **G9**, L53 (1983)

[7] S. Yoshida, et al, Astropart. Phys. **3**, 105 (1995)

[8] R.N. Coy et al, *The Lateral Distribution of Extensive Air Showers Produced by Cosmic Rays above* 10^{19} *eV as Measured by Water-Cherenkov Detectors*, GAP Note GAP-96-030 (1996);
M.A. Lawrence et al, J. Phys. **G17**, 733 (1991)

[9] The parameterization of the lateral distribution function, $\rho_\theta(r)$, is as follows [8]:

$$\rho_\theta(r) \;=\; k \cdot r^{-(\eta + \frac{r}{4000\,m})} \qquad (r < 800m)$$

and

$$\rho_\theta(r) \;=\; k \cdot r^{-(\eta + \frac{r}{4000\,m})} \cdot (\frac{r}{800m})^{1.03} \qquad (r \geq 800m)$$

where r is the radial distance from the shower core and θ is the shower zenith angle. The normalization, k, is obtained from the shower energy, E_{shower}, and angle using the following relations:

$$E_{shower} \;=\; 7.04 \times 10^{17} eV \cdot \rho_0(600)^{1.018}$$

where $\rho_0(600)$ is the measured density (in VEMs) 600m from the shower core for vertical showers (*i.e.* $\theta = 0$). For showers at non-zero zenith angle the corresponding particle density is:

$$\rho_\theta(600) \;=\; \rho_0(600) \cdot e^{-(\frac{1018}{760} \cdot (1/cos\theta \;-\; 1))}$$

Finally, the radial exponent, η, is given by:

$$\eta \;=\; 3.49 \;-\; 1.29/cos\theta \;+\; 0.165 \cdot log_{10}(\frac{E_{shower}}{10^{17} eV})$$

[10] The uncertainty in the shower direction is related to an uncertainty in the shower energy through the empirical factor relating $\rho_\theta(r)$ and $\rho_0(r)$. This factor is a correction for the changing effective atmospheric depth of the ground array with zenith angle [3]. As noted in the text, the *shower depth* uncertainty is minimized for a given experiment by an appropriate choice of radius used to measure $\rho(r)$ for correlation with the shower energy. For the Haverah Park experiment with $r = 600$m the relationship between $\rho_\theta(r)$ and $\rho_0(r)$ is given in [9]. To a first approximation it results in a small contribution to the energy uncertainty for $\theta \leq 45°$. However the energy uncertainty grows rapidly for larger zenith angles and in these cases can not be ignored.

[11] We use the CERN program HFITV in the HBOOK software package, Rene Brun et al, *HBOOK – Statistics, Analysis and Histogramming*, 1993

[12] T. Kutter, et al, *Self Calibration of the Water Cherenkov Tanks: Experimental Results*, Pierre Auger Note GAP-97-025 (1997)

Table 1: Parameters/variables in Auger Ground Array Simulation. The *default* value of each parameter/variable is underlined.

Parameter/variable	Range of values
Shower energy ($\times 10^{19}$ eV)	1, 2, <u>5</u>, 10, 20
Shower zenith angle (degrees)	0, 15, <u>30</u>, 45
(Hexagonal) tank separation, $d_{hexagon}$ (meters)	1300, 1400, <u>1500</u>, 1600, 1700
Maximum tank signal, N_{max} (VEM)	1000, <u>2000</u>, 5000
Minimum signal, N_{min} (VEM)	0.36, <u>0.9</u>, 2.25
Statistical significance factor, f_s Special study: (cf. Fig. 4.2 Ref. [2])	0.2, <u>0.4</u>, 0.6 $r < 60$m: $f_s = 0.02$ $60 \leq r < 1500$m: $f_s = 0.5 \cdot \frac{r}{1500m}$ $r \geq 1500$m: $f_s = 0.5 + 0.04 \cdot \frac{r-1500m}{500m}$
Gain uncertainty, σ_g (%)	0., <u>2.5</u>, 5.
Closest tank cut, d_{cut} (meters)	200, <u>250</u>, 300

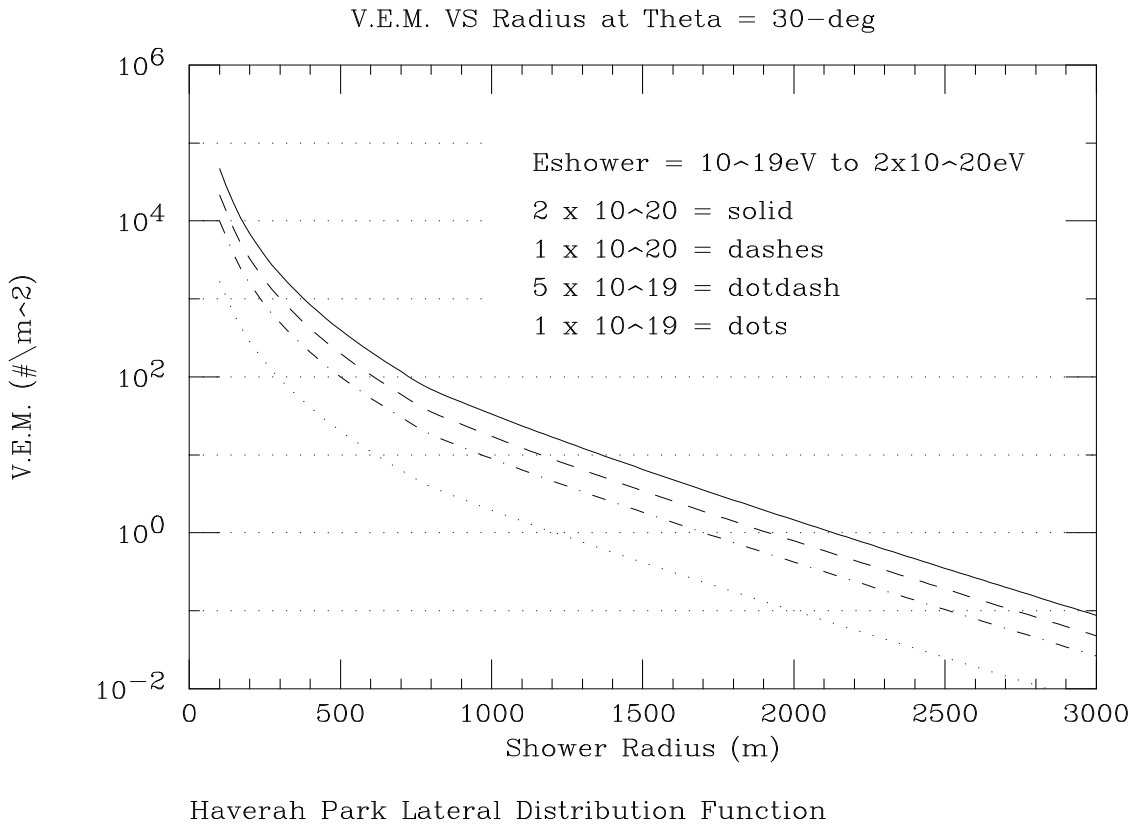

Fig. 1: Haverah Park lateral distribution function in units of Vertical Equivalent Muons.

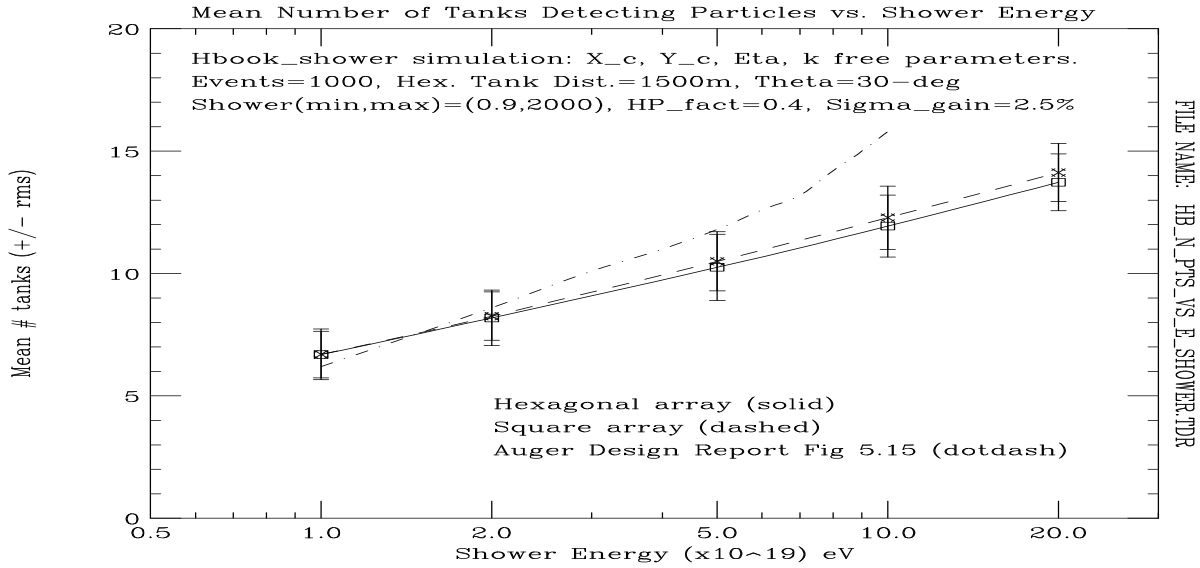

Fig. 2a: Average number of water Cherenkov tanks used in the ldf fit for both hexagonal and square geometries of the ground array. Only tanks with signal, N, between $N_{max} \geq N \geq N_{min}$ are included.

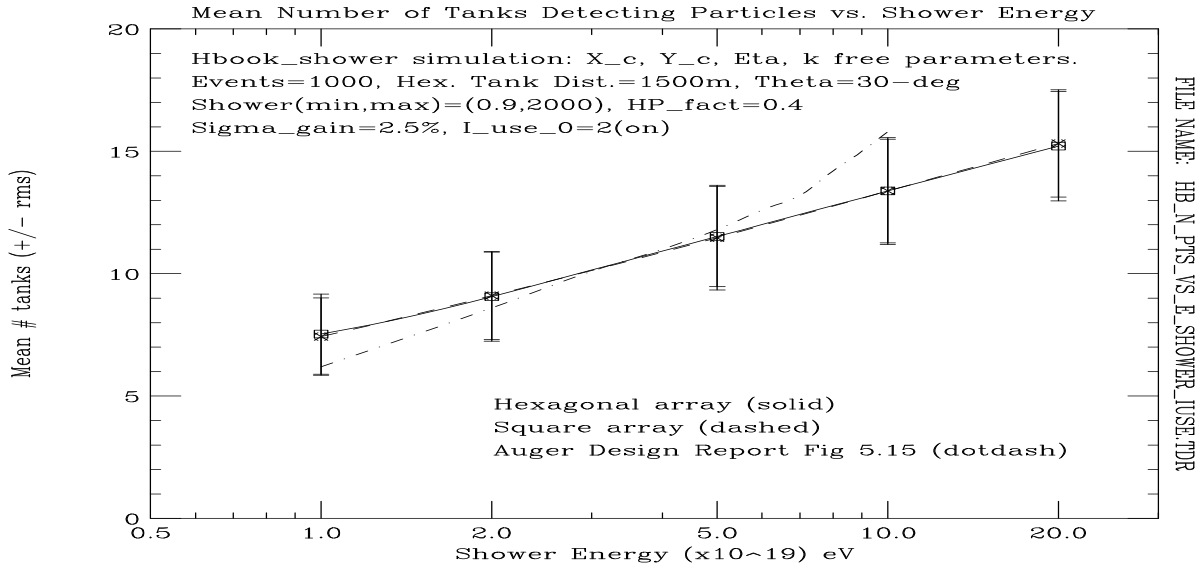

Fig. 2b: Average number of water Cherenkov tanks used in the ldf fit for both hexagonal and square geometries of the ground array. Tanks were included if the signal, N, was between $N_{max} \geq N \geq N_{min}$ or if the tank distance from the shower core was less than the maximum distance to a tank that passed the $N \geq N_{min}$ selection.

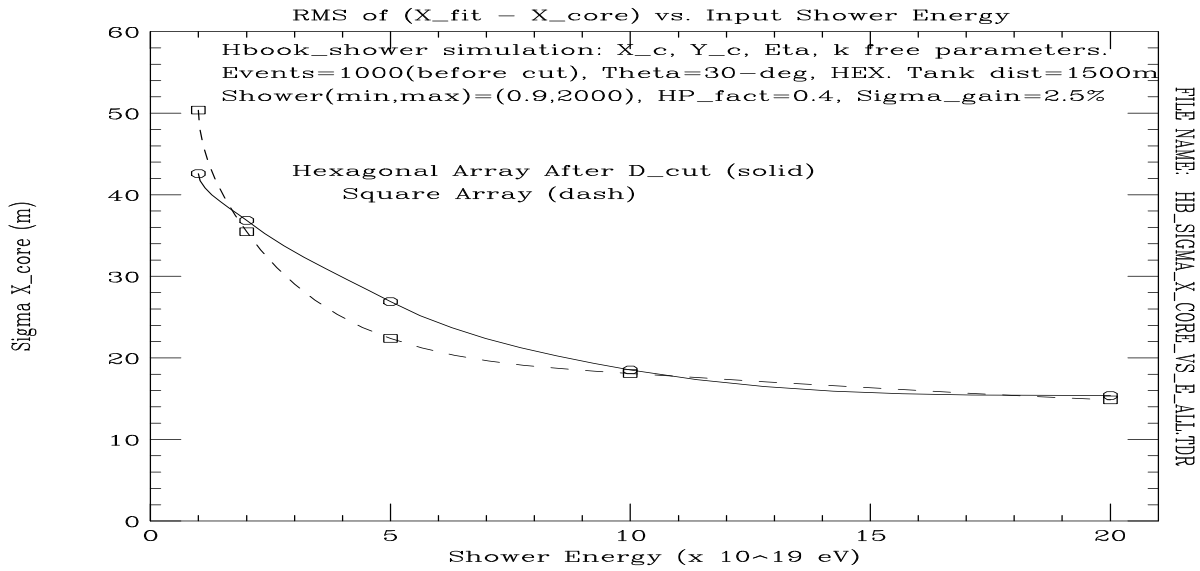

Fig. 3a: Uncertainty in fitted shower core location for both hexagonal and square geometries as a function of the shower energy. Tanks were included if the signal, N, was between $N_{max} \geq N \geq N_{min}$. The hexagonal array data exclude events with shower cores within a distance, d_{cut}, of a tank.

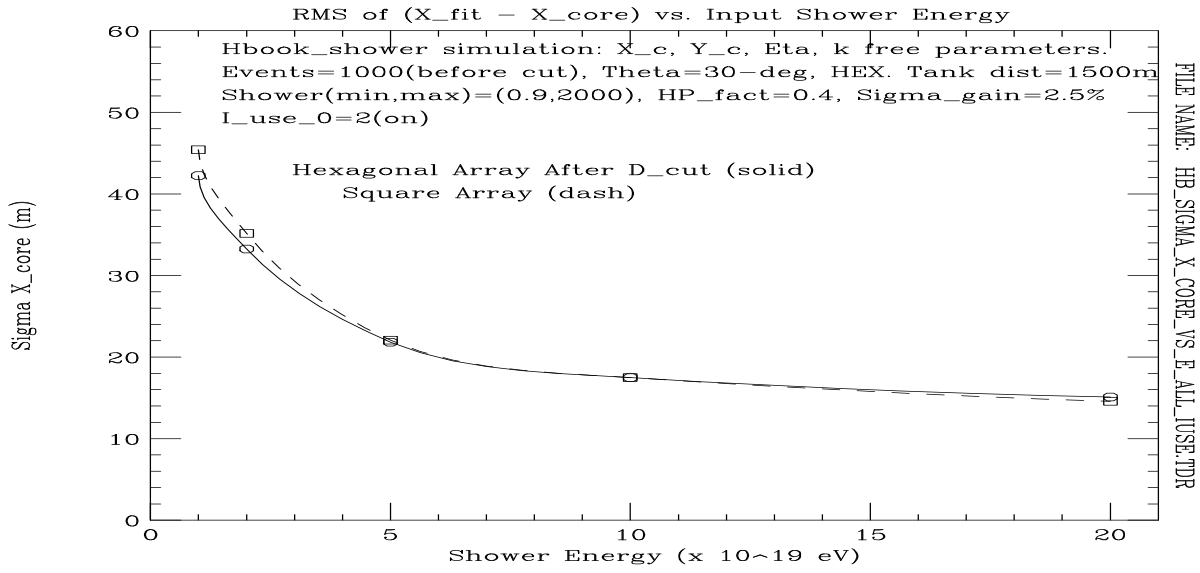

Fig. 3b: Uncertainty in fitted shower core location for both hexagonal and square geometries as a function of the shower energy. The hexagonal array data exclude events with shower cores within a distance, d_{cut}, of a tank. Tanks were included if the signal, N, was between $N_{max} \geq N \geq N_{min}$ or if the tank distance from the shower core was less than the maximum distance to a tank that passed the $N \geq N_{min}$ selection.

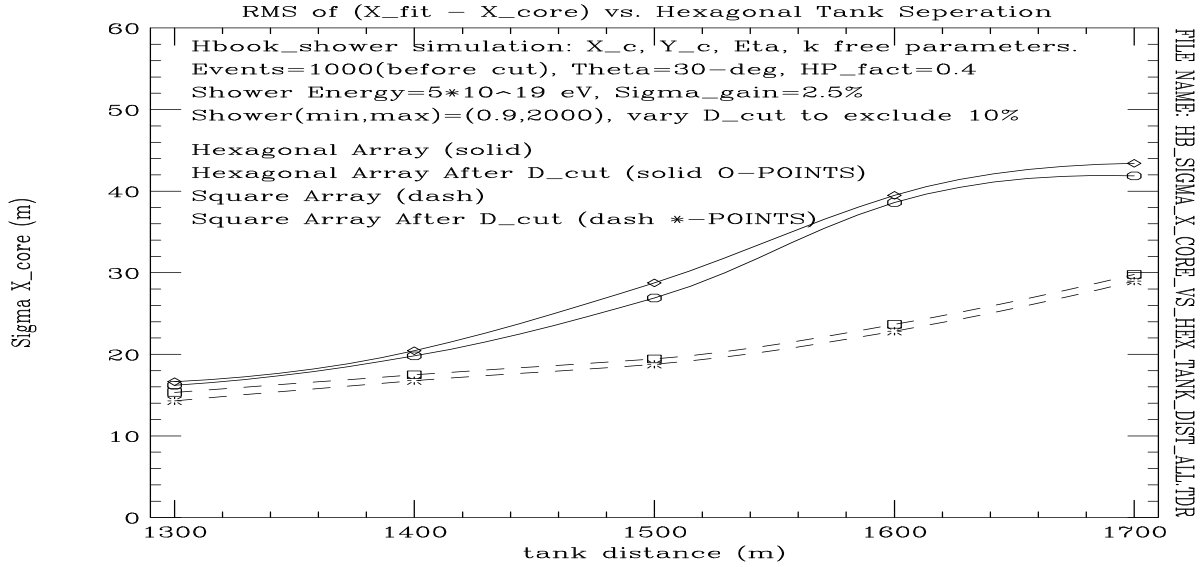

Fig. 4a: Uncertainty in fitted shower core location for both hexagonal and square geometries as a function of the tank separation distance, $d_{hexagon}$. Tanks were included if the signal, N, was between $N_{max} \geq N \geq N_{min}$. Results are shown with, and without, the requirement that reconstructed shower cores are outside a distance, d_{cut}, of a tank.

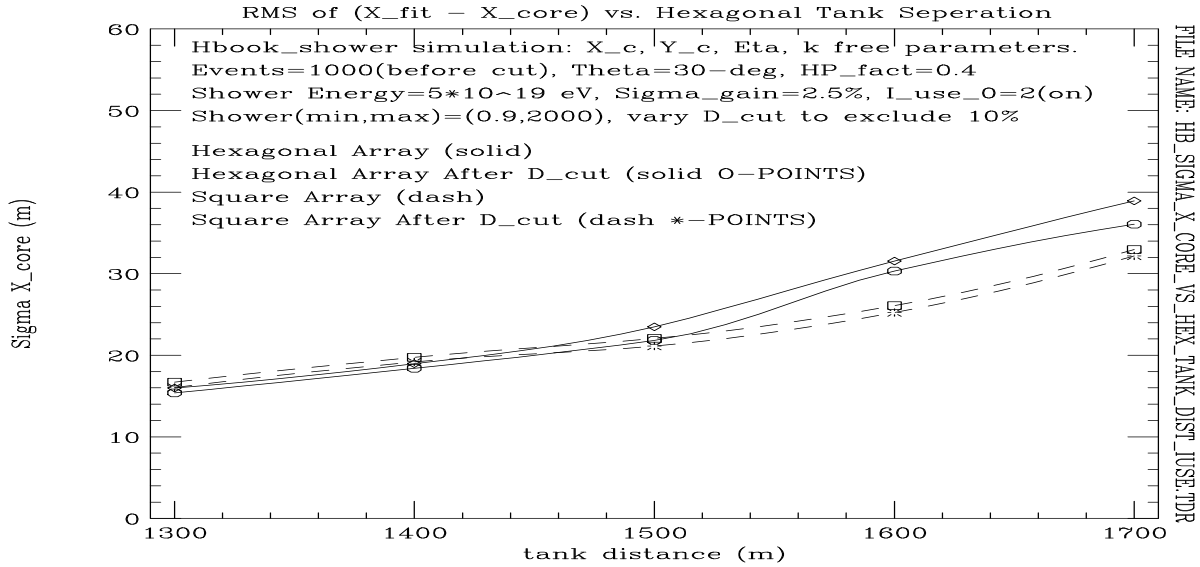

Fig. 4b: Uncertainty in fitted shower core location for both hexagonal and square geometries as a function of the tank separation distance, $d_{hexagon}$. Results are shown with, and without, the requirement that reconstructed shower cores are outside a distance, d_{cut}, of a tank. Tanks were included if the signal, N, was between $N_{max} \geq N \geq N_{min}$ or if the tank distance from the shower core was less than the maximum distance to a tank that passed the $N \geq N_{min}$ selection.

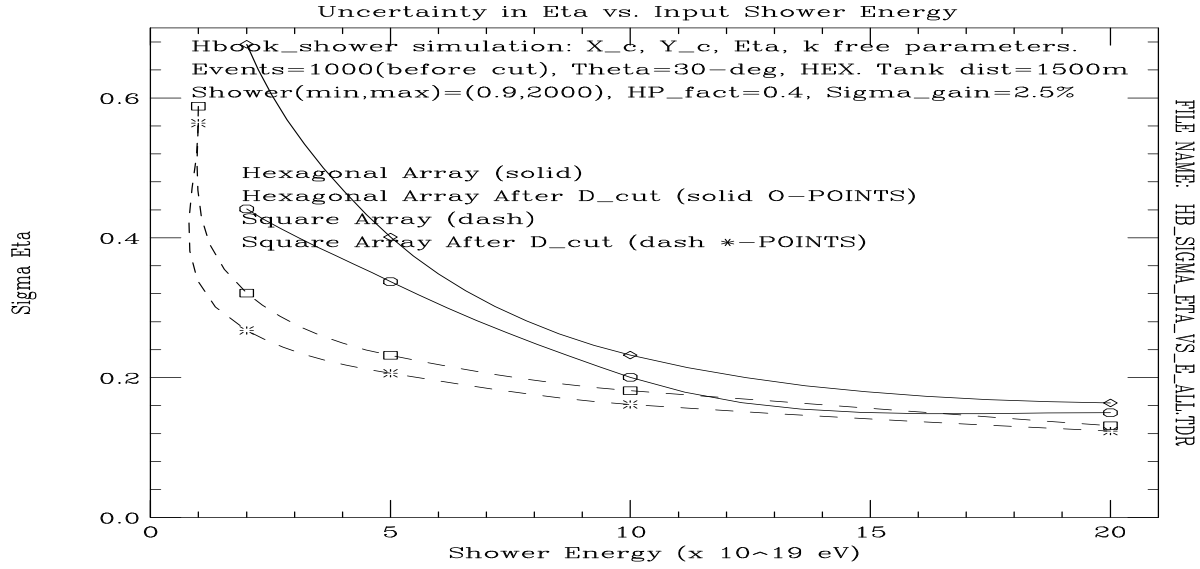

Fig. 5a: Uncertainty in radial exponent, η, of reconstructed shower ldf for both hexagonal and square geometries as a function of the shower energy. Tanks were included if the signal, N, was between $N_{max} \geq N \geq N_{min}$. Results are shown with, and without, the requirement that reconstructed shower cores are outside a distance, d_{cut}, of a tank.

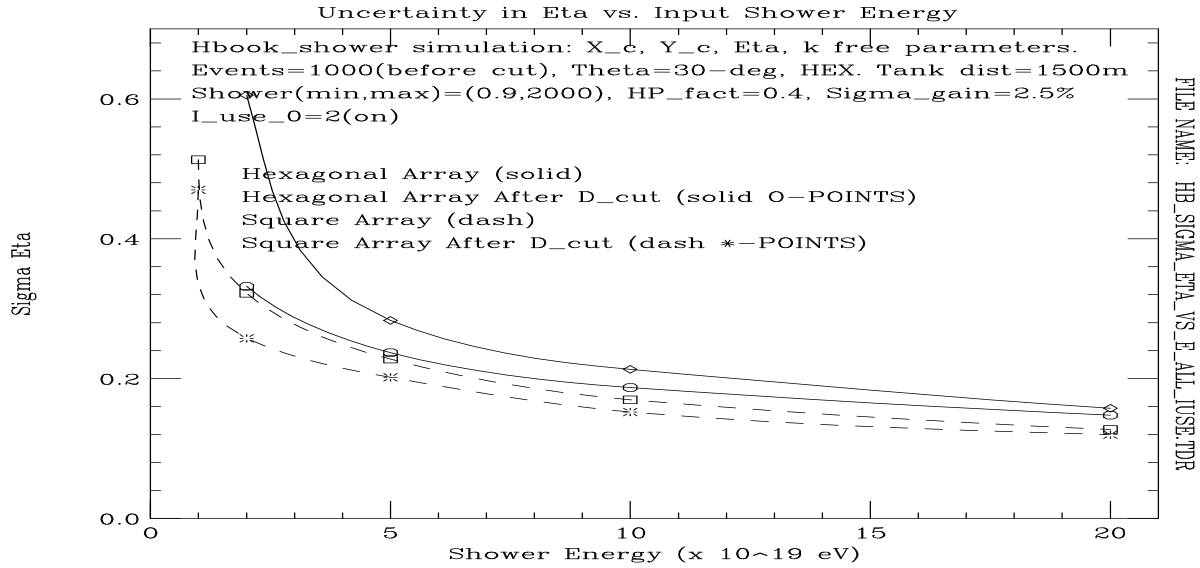

Fig. 5b: Uncertainty in radial exponent, η, of reconstructed shower ldf for both hexagonal and square geometries as a function of the shower energy. Results are shown with, and without, the requirement that reconstructed shower cores are outside a distance, d_{cut}, of a tank. Tanks were included if the signal, N, was between $N_{max} \geq N \geq N_{min}$ or if the tank distance from the shower core was less than the maximum distance to a tank that passed the $N \geq N_{min}$ selection.

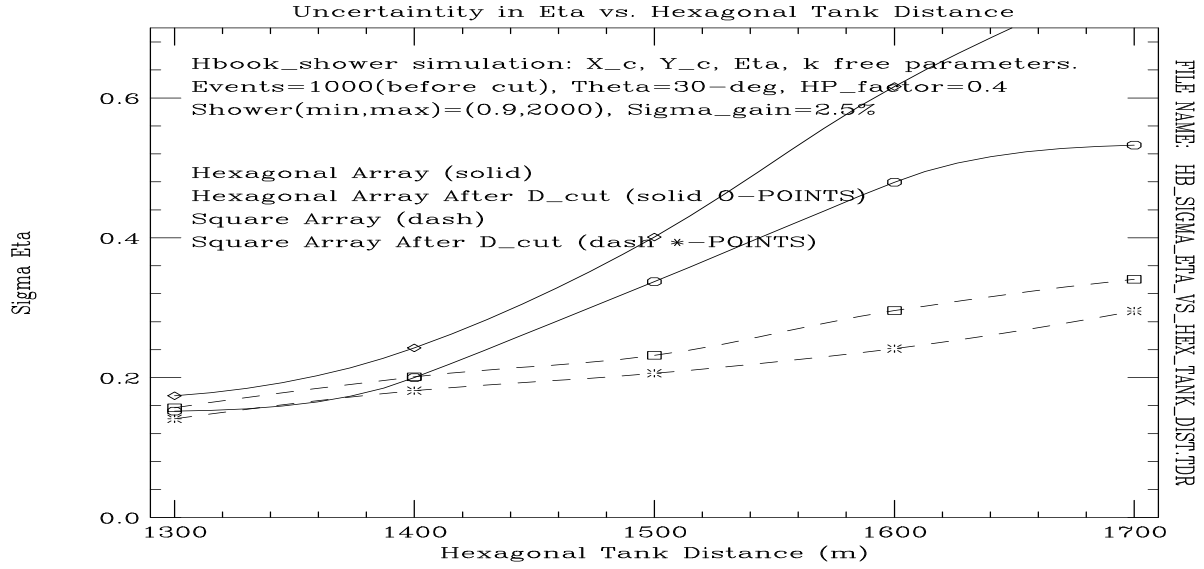

Fig. 6a: Uncertainty in radial exponent, η, for both hexagonal and square geometries as a function of the tank separation distance, $d_{hexagon}$. Tanks were included if the signal, N, was between $N_{max} \geq N \geq N_{min}$. Results are shown with, and without, the requirement that reconstructed shower cores are outside a distance, d_{cut}, of a tank.

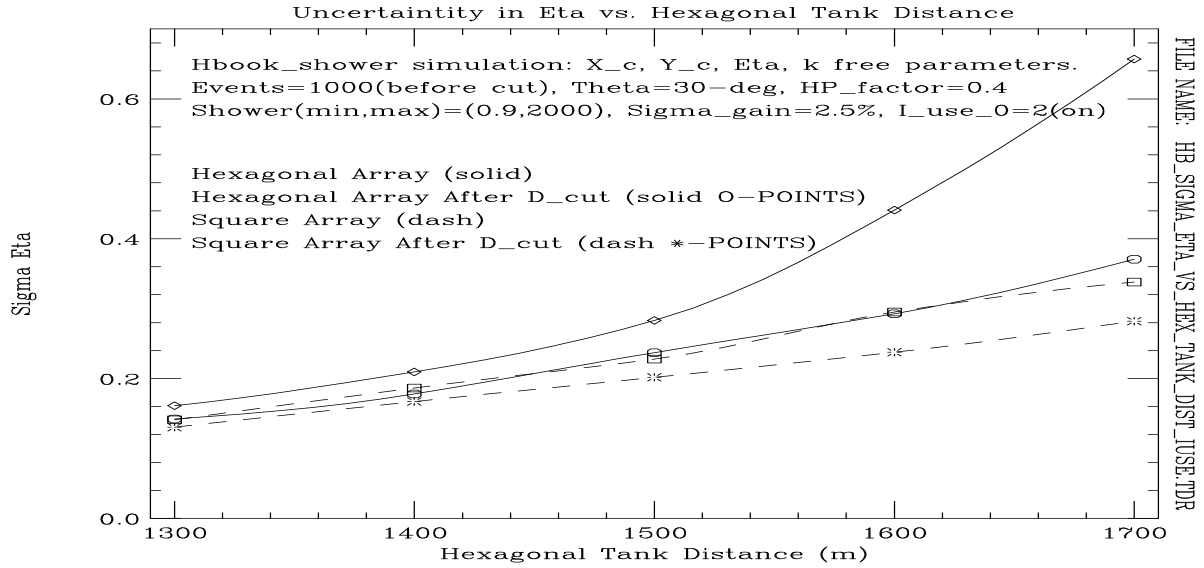

Fig. 6b: Uncertainty in radial exponent, η, for both hexagonal and square geometries as a function of the tank separation distance, $d_{hexagon}$. Results are shown with, and without, the requirement that reconstructed shower cores are outside a distance, d_{cut}, of a tank. Tanks were included if the signal, N, was between $N_{max} \geq N \geq N_{min}$ or if the tank distance from the shower core was less than the maximum distance to a tank that passed the $N \geq N_{min}$ selection.

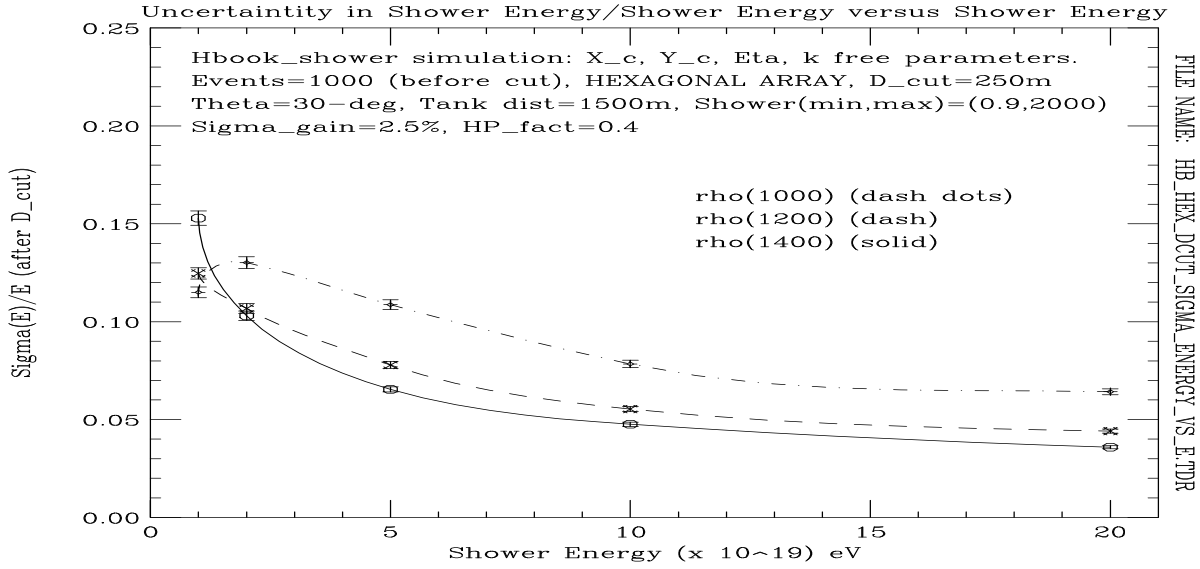

Fig. 7a: Normalized uncertainty in reconstructed shower energy for the hexagonal geometry of the ground array as a function of the shower energy. Tanks were included if the signal, N, was between $N_{max} \geq N \geq N_{min}$. Results are shown with, and without, the requirement that reconstructed shower cores are outside a distance, d_{cut}, of a tank.

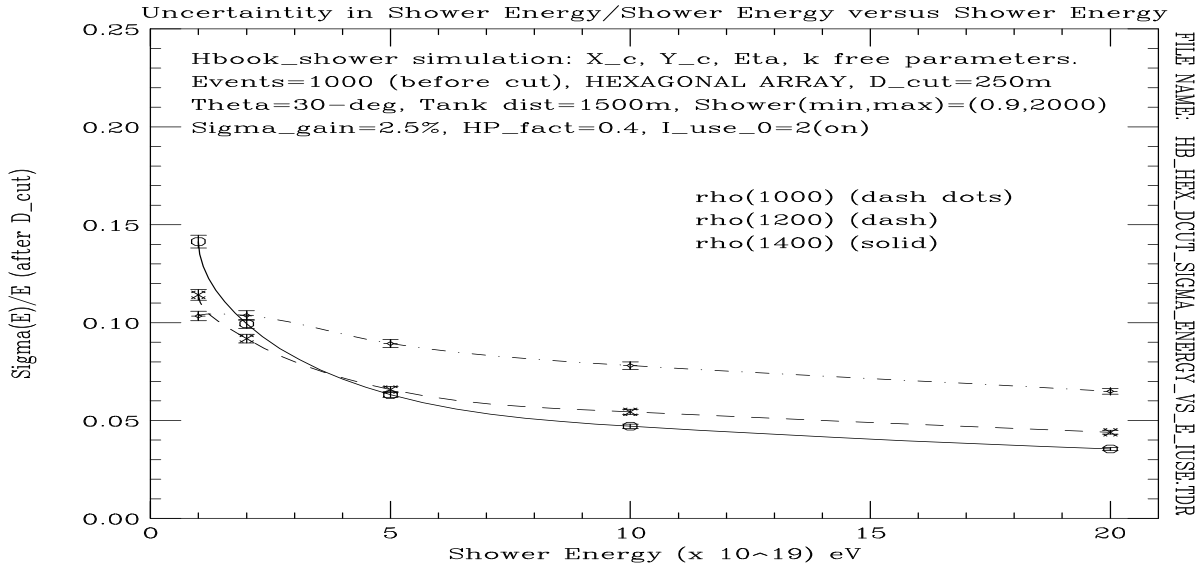

Fig. 7b: Normalized uncertainty in reconstructed shower energy for the hexagonal geometry of the ground array as a function of the shower energy. Results are shown with, and without, the requirement that reconstructed shower cores are outside a distance, d_{cut}, of a tank. Tanks were included if the signal, N, was between $N_{max} \geq N \geq N_{min}$ or if the tank distance from the shower core was less than the maximum distance to a tank that passed the $N \geq N_{min}$ selection.

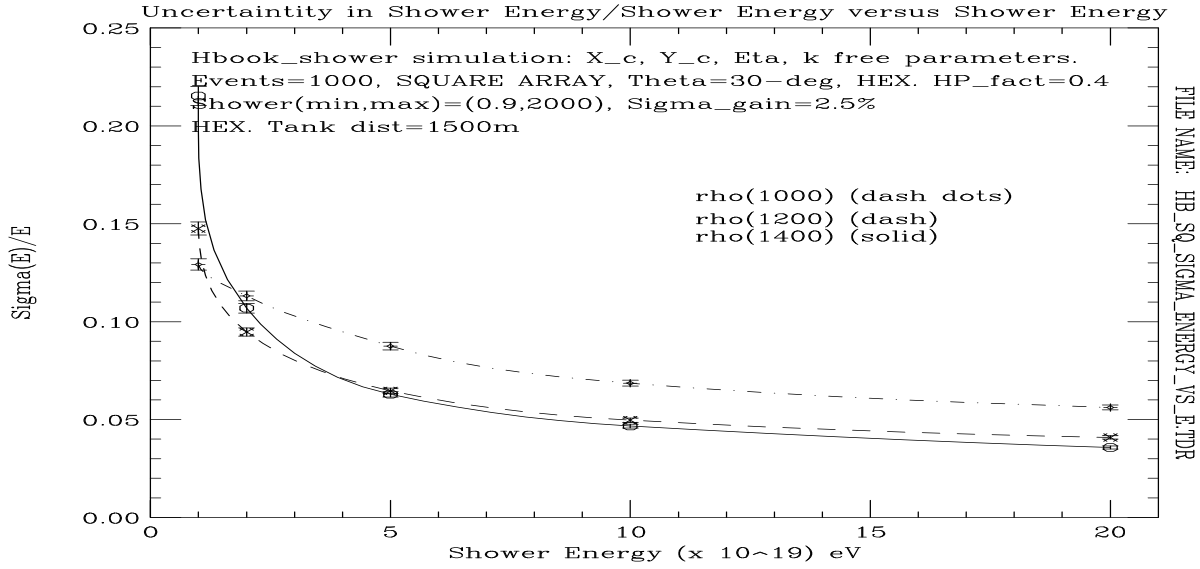

Fig. 7c: Normalized uncertainty in reconstructed shower energy for the square geometry of the ground array as a function of the shower energy. Tanks were included if the signal, N, was between $N_{max} \geq N \geq N_{min}$. Results are shown with, and without, the requirement that reconstructed shower cores are outside a distance, d_{cut}, of a tank.

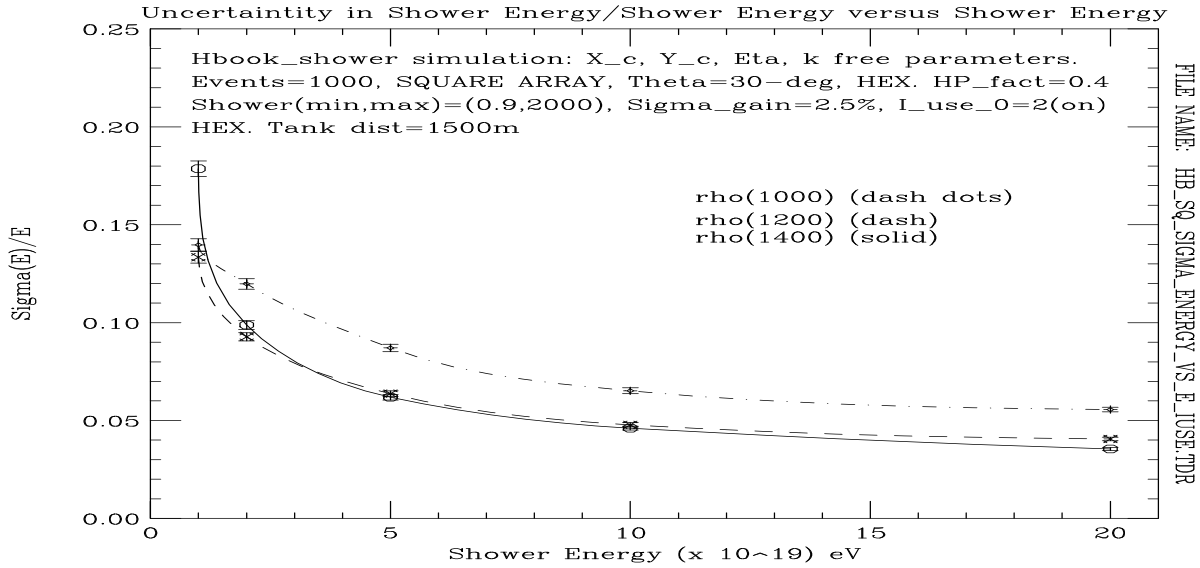

Fig. 7d: Normalized uncertainty in reconstructed shower energy for the square geometry of the ground array as a function of the shower energy. Results are shown with, and without, the requirement that reconstructed shower cores are outside a distance, d_{cut}, of a tank. Tanks were included if the signal, N, was between $N_{max} \geq N \geq N_{min}$ or if the tank distance from the shower core was less than the maximum distance to a tank that passed the $N \geq N_{min}$ selection.

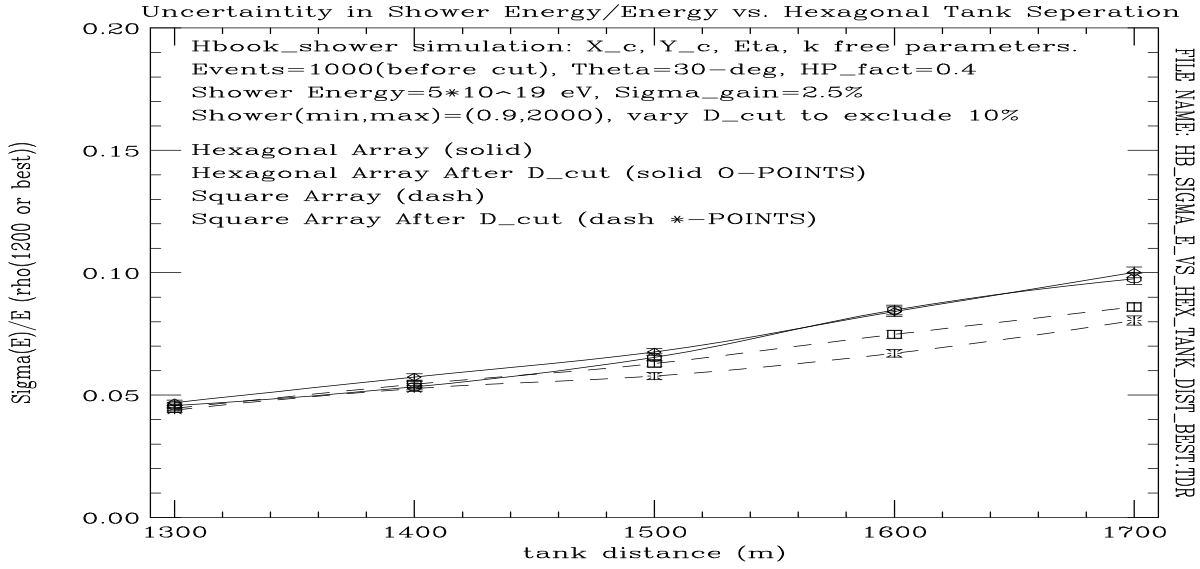

Fig. 8a: Normalized uncertainty in reconstructed shower energy for both hexagonal and square geometries as a function of the tank separation distance, $d_{hexagon}$. Tanks were included if the signal, N, was between $N_{max} \geq N \geq N_{min}$. Results are shown with, and without, the requirement that reconstructed shower cores are outside a distance, d_{cut}, of a tank.

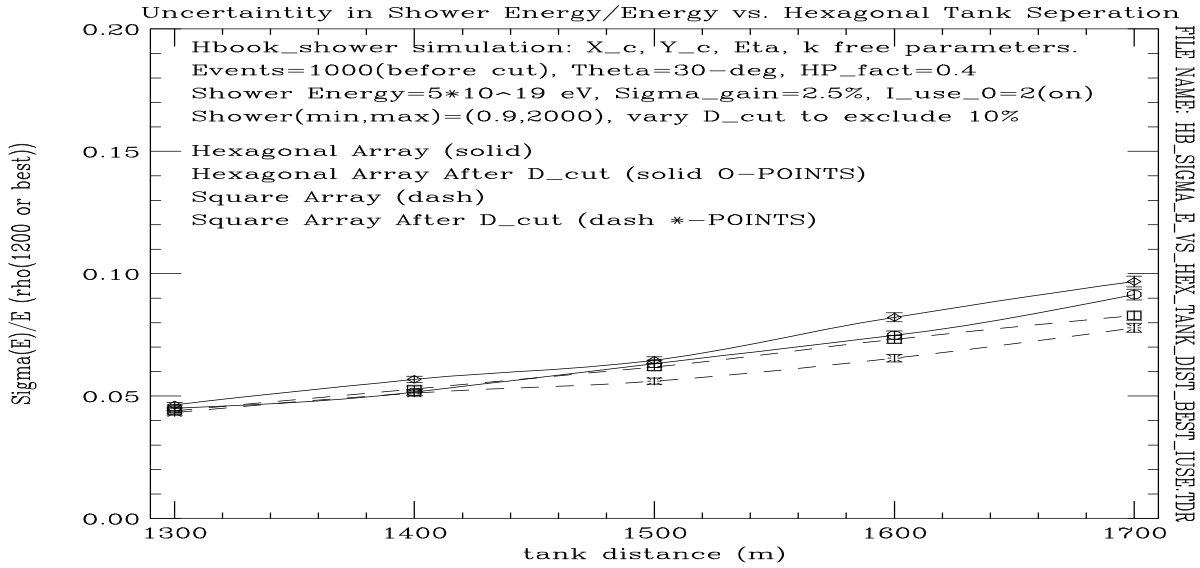

Fig. 8b: Normalized uncertainty in reconstructed shower energy for both hexagonal and square geometries as a function of the tank separation distance, $d_{hexagon}$. Results are shown with, and without, the requirement that reconstructed shower cores are outside a distance, d_{cut}, of a tank. Tanks were included if the signal, N, was between $N_{max} \geq N \geq N_{min}$ or if the tank distance from the shower core was less than the maximum distance to a tank that passed the $N \geq N_{min}$ selection.

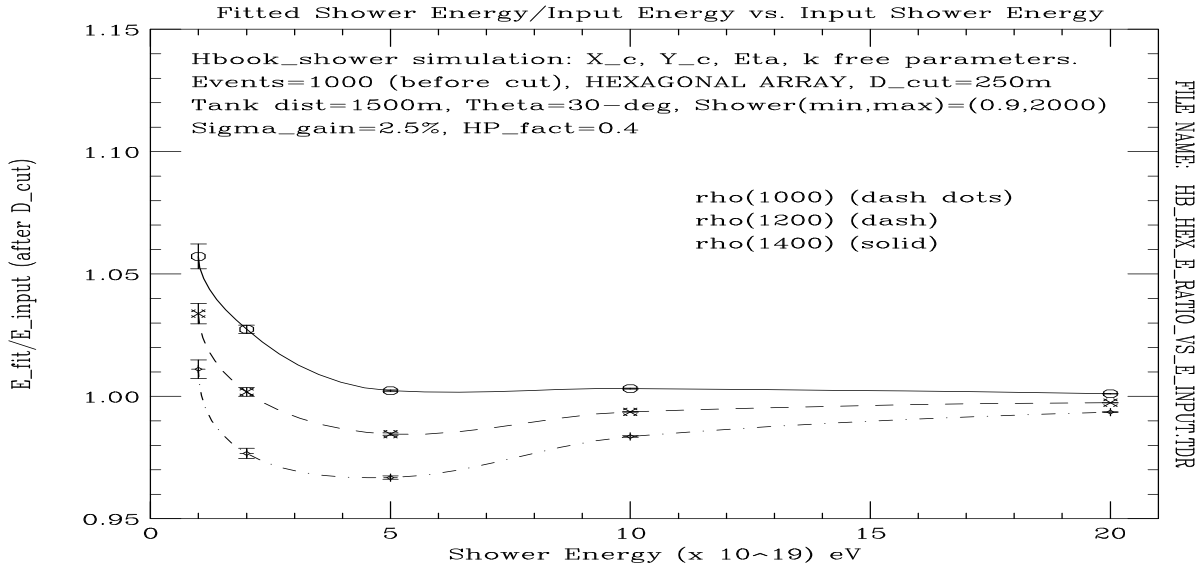

Fig. 9a: Ratio of E_{fit}/E_{shower} for the hexagonal geometry of the ground array as a function of the shower energy. Tanks were included if the signal, N, was between $N_{max} \geq N \geq N_{min}$. Results are shown with, and without, the requirement that reconstructed shower cores are outside a distance, d_{cut}, of a tank.

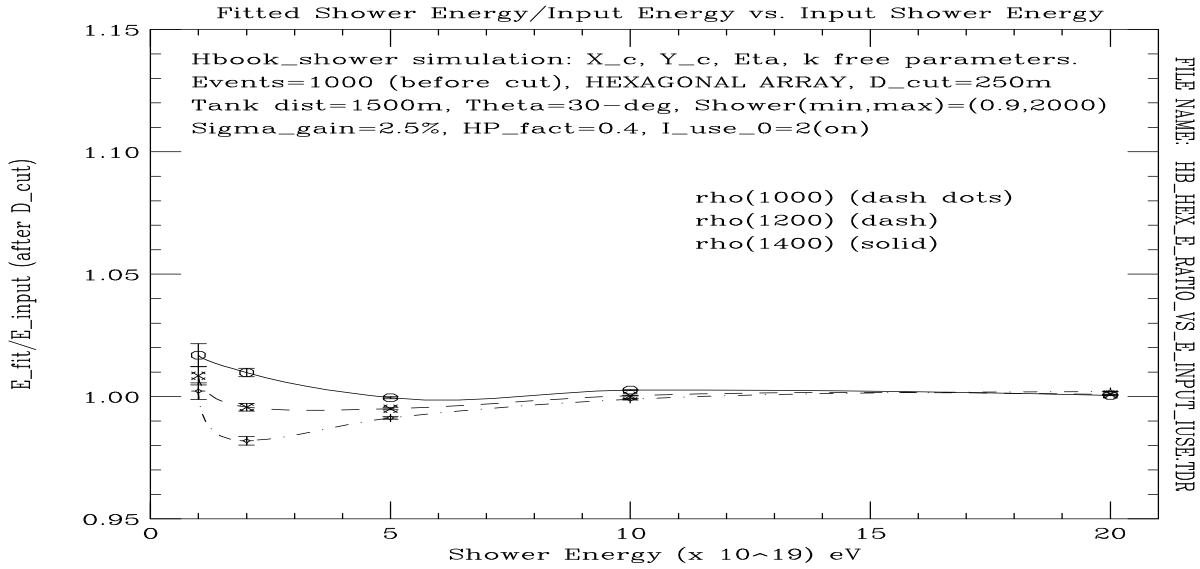

Fig. 9b: Ratio of E_{fit}/E_{shower} for the hexagonal geometry of the ground array as a function of the shower energy. Results are shown with, and without, the requirement that reconstructed shower cores are outside a distance, d_{cut}, of a tank. Tanks were included if the signal, N, was between $N_{max} \geq N \geq N_{min}$ or if the tank distance from the shower core was less than the maximum distance to a tank that passed the $N \geq N_{min}$ selection.

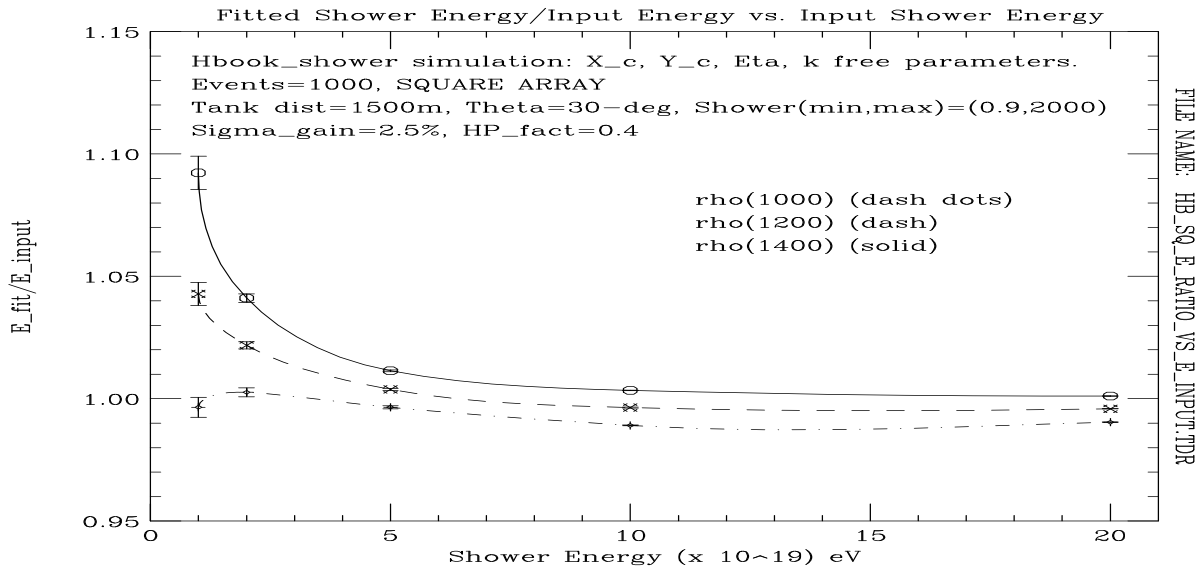

Fig. 9c: Ratio of E_{fit}/E_{shower} for the square geometry of the ground array as a function of the shower energy. Tanks were included if the signal, N, was between $N_{max} \geq N \geq N_{min}$. Results are shown with, and without, the requirement that reconstructed shower cores are outside a distance, d_{cut}, of a tank.

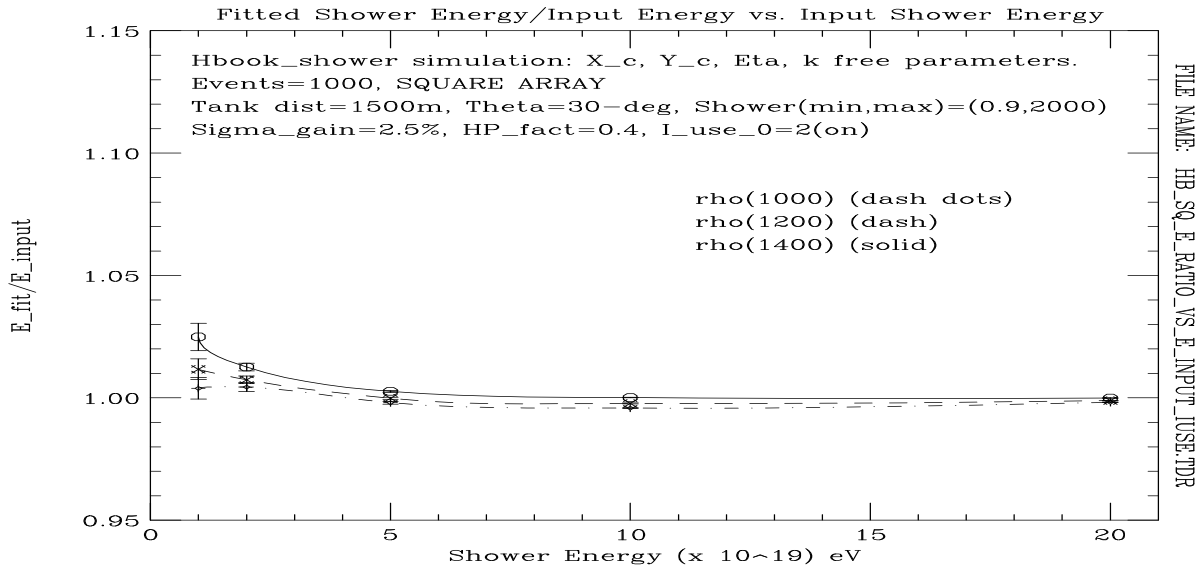

Fig. 9d: Ratio of E_{fit}/E_{shower} for the square geometry of the ground array as a function of the shower energy. Results are shown with, and without, the requirement that reconstructed shower cores are outside a distance, d_{cut}, of a tank. Tanks were included if the signal, N, was between $N_{max} \geq N \geq N_{min}$ or if the tank distance from the shower core was less than the maximum distance to a tank that passed the $N \geq N_{min}$ selection.